ELSEVIER

Fluid Phase Equilibria 183–184 (2001) 53–64

FLUID PHASE EQUILIBRIA

www.elsevier.com/locate/fluid

A crossover equation of state for associating fluids

S.B. Kiselev [a,*], J.F. Ely [a], H. Adidharma [b], M. Radosz [b]

[a] *Chemical Engineering Department, Colorado School of Mines, Golden, CO 80401-1887, USA*
[b] *Department of Chemical and Petroleum Engineering, University of Wyoming, Laramie, WY 82071-3295, USA*

Abstract

In this work we extend the crossover (CR) modification of the statistical-associating-fluid-theory (SAFT) equation of state (EOS), recently developed and applied for non-associating systems [Ind. Eng. Chem. Res. 38 (1999) 4993] to associating fluids. Unlike the previous crossover EOS that was based on the parametric linear model for the universal crossover function *Y*, the new CR SAFT EOS is based on Fisher's recent parametric sine model. This model can be extended into the metastable region and gives analytically connected van der Waals loops in the two-phase region. We show that for associating fluids the new CR SAFT EOS not only yields a better description of the PVT and VLE properties of fluids in the critical region, but also improves the representation of the entire thermodynamic surface. A comparison is made with experimental data for pure normal methanol, ethanol, propanol, butanol, pentanol, and hexanol in the one- and two-phase regions. The CR SAFT EOS reproduces the saturated pressure and liquid density data with an average absolute deviation (AAD) of about 1%. In the one-phase region, the CR SAFT equation represents the experimental values of pressure with an AAD less than 1% in the critical and supercritical region and the liquid densities with an AAD of about 2%.

Keywords: Associating fluids; Critical state; Crossover theory; Equation of state; *n*-Alkanols; Thermodynamic properties; Vapor–liquid equilibrium

1. Introduction

Fluids containing associating molecules are always of great interest from an industrial point of view and their thermophysical properties are needed for many practical applications. However, due to the existence of strong and highly directional attractive forces in associating fluids, only a few thermodynamic models available today can be used to represent such a fluid.

One successful approach that can be used to model associating fluids is the statistical associating fluid theory (SAFT) which is firmly based in statistical mechanical perturbation theory. For years, the SAFT equation of state has been applied to model associating fluids, including both pure components

* Corresponding author. Tel.: +1-303-273-3190; fax: +1-303-273-3730.
E-mail address: skiselev@mines.edu (S.B. Kiselev).

0378-3812/01/$20.00
PII: S0378-3812(01)00420-4

and mixtures [2–8]. These applications have shown that the SAFT equation of state can reliably capture the behavior of associating fluids over a wide range of conditions. Nevertheless, in its original form, this equation of state fails to give an accurate description of the fluids in the region close to the critical point due to the existence of the long-range density fluctuations.

A crossover SAFT EOS for non-associating fluids which incorporates the long-range density fluctuations and reproduces the asymptotic scaling laws in the critical region was developed recently by Kiselev and Ely [1,9]. In the present paper we continue study initiated by Kiselev and Ely for *n*-alkanes [1] and refrigerants and refrigerant mixtures [9] and develop a crossover SAFT EOS for *n*-alkanols. The equation of state was tested against experimental VLE and PVT data for methanol, ethanol, propan-ol-1, butan-ol-1, pentan-ol-1, and hexan-ol-1.

2. SAFT equation of state

The SAFT equation of state is defined in terms of the residual Helmholtz energy per mole, a^{res}. For associating molecules, the molar residual Helmholtz energy consists of three terms [3]:

$$\frac{a^{\mathrm{res}}}{RT} = \tilde{a}^{\mathrm{res}} = \tilde{a}^{\mathrm{seg}} + \tilde{a}^{\mathrm{chain}} + \tilde{a}^{\mathrm{assoc}} \tag{1}$$

where $\tilde{a}^{\mathrm{seg}}$ is the Helmholtz energy due to segment–segment interactions, and is considered to be the reference term; $\tilde{a}^{\mathrm{chain}}$ the incremental Helmholtz energy due to chain formation; and $\tilde{a}^{\mathrm{assoc}}$ is the incremental Helmholtz energy due to association. A tilde ($\sim$) in this work means a dimensionless form of a variable.

The segment contribution is given by

$$\tilde{a}^{\mathrm{seg}} = m(\tilde{a}_o^{\mathrm{hs}} + \tilde{a}_o^{\mathrm{disp}}) \tag{2}$$

where m is the number of segments per molecule and $\tilde{a}_o^{\mathrm{hs}}$ is the Helmholtz energy of hard-sphere fluids per segment given by Carnahan–Starling [10]:

$$\tilde{a}_o^{\mathrm{hs}} = \frac{4\eta - 3\eta^2}{(1-\eta)^2} \tag{3}$$

In Eq. (3), η is the reduced density (segment packing fraction or volume fraction of segment) defined as

$$\eta = \frac{1}{6}\pi N_{\mathrm{Av}} \rho m d^3 \tag{4}$$

where N_{Av} is Avogadro's number, ρ the molar density and d is the effective diameter of the hard spherical segment (the temperature-dependent segment diameter). Using the inverted square-well potential, Chen and Kreglewski [11] expressed d as

$$d = \sigma\left[1 - C\exp\left(\frac{-3u^0}{kT}\right)\right] \tag{5}$$

where σ is the center-to-center distance between two segments at which the pair potential of the real fluid is zero (the temperature-independent segment diameter), k the Boltzmann constant, $C = 0.12$ for all fluids in this work, and u^0/k is the temperature-independent well depth of the square-well potential. The

temperature-independent segment diameter, σ is related to the temperature-independent segment molar volume in a closed-packed arrangement defined per mole of segments:

$$v^{00} = \frac{\pi}{6}\frac{N_{\mathrm{Av}}}{\tau}\sigma^3 \tag{6}$$

where $\tau = \sqrt{2}\pi/6$.

The dispersion part in Eq. (2), $\tilde{a}_o^{\mathrm{disp}}$, is given by [11]:

$$\tilde{a}_o^{\mathrm{disp}} = \sum_i \sum_j D_{ij} \left[\frac{u}{kT}\right]^i \left[\frac{\eta}{\tau}\right]^j \tag{7}$$

where D_{ij}s are universal constants and u is the temperature-dependent well depth defined as

$$u = u^0 \left(1 + \frac{e}{kT}\right) \tag{8}$$

Here, e/k is a constant that is related to Pitzer's acentric factor and the critical temperature, but since the energy parameter is for segments rather than for molecules, $e/k = 10$ for SAFT molecules [3].

The chain contribution, $\tilde{a}^{\mathrm{chain}}$ in Eq. (1) is related to the radial distribution function of the hard-sphere fluid at contact, $g^{\mathrm{hs}}(d)$, as follows:

$$\tilde{a}^{\mathrm{chain}} = -(m-1)\ln g^{\mathrm{hs}}(d) \tag{9}$$

where

$$g^{\mathrm{hs}}(d) = \frac{2-\eta}{2(1-\eta)^3} \tag{10}$$

The association contribution, $\tilde{a}^{\mathrm{assoc}}$ in Eq. (1), derived on the basis of Wertheim's thermodynamic perturbation theory, is given by

$$\tilde{a}^{\mathrm{assoc}} = \sum_{A\in\Gamma}\left(\ln X^A - \frac{X^A}{2}\right) + \frac{n(\Gamma)}{2} \tag{11}$$

where $n(\Gamma)$ is the number of association sites on the molecule and X^A is the fraction of molecules that are not bonded at site A. The expression for X^A is also obtained from Wertheim's theory:

$$X^A = \left(1 + N_{\mathrm{Av}}\rho \sum_{B\in\Gamma} X^B \Delta^{AB}\right)^{-1} \tag{12}$$

where Δ^{AB} is the association strength given by

$$\Delta^{AB} = \sigma^3 \kappa^{AB}\left[\exp\left(\frac{\varepsilon^{AB}}{kT}\right) - 1\right] g^{\mathrm{hs}}(d) \tag{13}$$

where ε^{AB} is the well depth of the site–site potential and $\sigma^3\kappa^{AB}$ is a measure of the volume available for bonding.

To obtain specific expressions for $\tilde{a}^{\mathrm{assoc}}$ and X^A, one has to hypothesize the number of association sites and make simplifying approximations for the association strength of site–site interactions. Following

Huang and Radosz [3], in this work a *n*-alkanol is modeled as an associating chain molecule with two association sites, i.e. model 2B. Thus, the total number of SAFT parameters for this type of associating fluid is five, i.e. m, v^{00} (or σ), u^0/k, ε/k, and κ^{AB}. The last two parameters are specifically from the association term.

We note that in applying the crossover model, the equation of state's classical critical molar density and temperature, i.e. ρ_{0c} and T_{0c}, are required and these are obtained by solving the criticality conditions

$$\left(\frac{\partial P}{\partial \rho}\right)_{T_{0c}} = \left(\frac{\partial^2 P}{\partial \rho^2}\right)_{T_{0c}} = 0 \tag{14}$$

where P is the pressure. Once ρ_{0c} and T_{0c} are known, the critical pressure P_{0c} can be obtained.

3. Crossover SAFT equation

In order to obtain the crossover (CR) SAFT EOS, one needs first to represent the classical expression for the dimensionless Helmholtz free energy in the form [1]

$$\tilde{a}(T, v) = \Delta\tilde{a}(\Delta T, \Delta v) - \Delta v \tilde{P}_0(T) + \tilde{a}_0^{\text{res}}(T) + \tilde{a}_0(T) \tag{15}$$

where the critical part of the Helmholtz free energy

$$\Delta\tilde{a}(\Delta T, \Delta v) = \tilde{a}^{\text{res}}(\Delta T, \Delta v) - \tilde{a}^{\text{res}}(\Delta T, 0) - \ln(\Delta v + 1) + \Delta v \tilde{P}_0(\Delta T) \tag{16}$$

is expressed as a function of the dimensionless deviations of the temperature $\Delta T = T/T_{0c} - 1$ and the molar volume $\Delta v = v/v_{0c} - 1$ from the classical critical temperature T_{0c} and the classical molar volume v_{0c}. $\tilde{P}_0(T) = P(T, v_{0c})v_{0c}/RT$ and $\tilde{a}_0^{\text{res}}(T) = \tilde{a}_0^{\text{res}}(T, v_{0c})$ are the dimensionless pressure and the residual Helmholtz energy along the critical isochore, and $\tilde{a}_0(T)$ the dimensionless temperature-dependent ideal gas part. The next step is to replace ΔT and Δv in singular part $\Delta\tilde{a}(\Delta T, \Delta v)$ with their renormalized values

$$\bar{\tau} = \tau \Upsilon^{-\alpha/2\Delta_1} + (1 + \tau)\Delta\tau_c \Upsilon^{2(2-\alpha)/3\Delta_1} \tag{17}$$

$$\Delta\bar{\eta} = \Delta\eta \Upsilon^{(\gamma-2\beta)/4\Delta_1} + (1 + \Delta\eta)\Delta\eta_c \Upsilon^{(2-\alpha)/2\Delta_1} \tag{18}$$

so that $\Delta T \to \bar{\tau}$ and $\Delta v \to \Delta\bar{\eta}$ in Eq. (16), where $\tau = T/T_c - 1$ is the dimensionless deviation of the temperature from the real critical temperature T_c, $\Delta\eta = v/v_c - 1$ the dimensionless deviations of the molar volume form the real critical molar volume v_c, and the factors $\Delta\tau_c = \Delta T_c/T_{0c} = (T_c - T_{0c})/T_{0c}$ and $\Delta\eta_c = \Delta v_c/v_{0c} = (v_c - v_{0c})/v_{0c}$ are the dimensionless shifts of the critical parameters.

In Eqs. (17) and (18) $\gamma = 1.24$, $\beta = 0.325$, $\alpha = 2 - \gamma - 2\beta = 0.11$, and $\Delta_1 = 0.51$ are the universal non-classical critical exponents, and the crossover function Υ can be represented in the parametric form [1]

$$\Upsilon(q) = \left(\frac{q}{1+q}\right)^{2\Delta_1} \tag{19}$$

Physically, the parametric variable q is a renormalized distance from the critical point. In our previous work [1], q was found from a solution of the parametric linear model (LM). In this study, following the

recent work of Kiselev and Ely [9],we find the parametric variable q from a solution of the crossover parametric sine model

$$\left(q^2 - \frac{\tau}{G_i}\right)\left[1 - \frac{p^2}{4b^2}\left(1 - \frac{\tau}{q^2 G_i}\right)\right] = \frac{b^2}{{G_i}^{2\beta}}\left(\frac{q}{1+q}\right)^{2(1-2\beta)} \times\{\Delta\eta[1 + v_1\Delta\eta^2\exp(-\delta_1\Delta\eta)] + d_1\tau(1-2\tau)\}^2 \quad (20)$$

where G_i is the Ginzburg number for the fluid of interest, v_1 and d_1 the system-dependent parameters, $\delta_1 = 8.5$ is a constant, and the parameters p^2 and b^2 can be set equal to the universal LM parameter $b^2_{\mathrm{LM}} = 1.359$ [9]. The linear-model crossover equation for the parametric variable q employed earlier by Kiselev et al. [1,12,13] is recaptured from Eq. (20) when the parameter $p^2 \to 0$.

Finally, the crossover expression for the Helmholtz free energy can be written in the form

$$\tilde{a}(T, v) = \Delta\tilde{a}(\bar{\tau}, \Delta\bar{\eta}) + \Delta v\tilde{P}_0(T) + \tilde{a}_0^{\mathrm{res}}(T) + \tilde{a}_0(T) - K(\tau^2) \quad (21)$$

where the kernel term $K(\tau^2)$ should be added in order to reproduce the asymptotic singular behavior of the isochoric heat capacity along the critical isochore [12]. Since the isochoric heat capacity is not considered in this work we set here $K(\tau^2) = 0$. The final crossover SAFT equation of state in this case reads

$$P(T, v) = \frac{RT}{v_{0\mathrm{c}}}\left[-\frac{v_{0\mathrm{c}}}{v_{\mathrm{c}}}\left(\frac{\partial\Delta\tilde{a}}{\partial\Delta\eta}\right)_T + \bar{P}_0(T)\right] \quad (22)$$

4. Comparison with experimental data

In the present work, we applied crossover SAFT EOS for the description of the PVT and VLE properties of *n*-alkanols in and far beyond the critical region. In addition to the original SAFT parameters m, v^{00}, u^0/k, ε/k, and κ in Eqs. (1)–(13), the crossover SAFT EOS for *n*-alkanols contains also the crossover parameters G_i, v_1 and d_1 in Eq. (20) for the parametric variable q. The parameters m, v^{00}, u^0/k, ε/k, and κ determine the classical critical parameters $T_{0\mathrm{c}}$, ρ_{0c}, and $P_{0\mathrm{c}}$ which, in general, do not coincide with the real experimental values T_{c}, ρ_{c}, and P_{c}. Thus, if one needs also to keep the real values of the critical temperature and density, the critical shifts in Eqs. (17) and (18), $\Delta\tau_c$ and $\Delta\eta_c$, should be considered as additional system-dependent parameters. The exact values of the critical temperature and density are highly needed for an accurate reproducing of the isochoric specific heat data in the nearest vicinity of the critical point, which are not considered here. Therefore, in the present work, following Kiselev and Ely [9] the critical shifts $\Delta\tau_c$ and $\Delta\eta_c$, and the parameter v_1 were represented as functions of the Ginzburg number

$$\Delta\tau_c = -\frac{\delta_\tau G_i}{1 + \delta_\tau G_i}, \quad (23)$$

$$\Delta\eta_c = -\frac{\delta_\rho G_i}{1 + \delta_\delta G_i} \quad (24)$$

$$v_1 = \frac{v_1^{(0)} + v_1^{(1)}}{G_i} \quad (25)$$

Table 1
System-dependent parameters for the crossover SAFT EOS

Parameter	Methanol	Ethanol	Propanol-1	Butanol-1	Pentanol-1	Hexanol-1
v^{00} (ml mol^{-1})	6.21528	5.66344	6.58931	8.03448	10.2215	12.1164
M	3.29388	5.13447	5.72886	6.03793	5.70949	5.63890
u^0/k (K)	152.775	154.067	161.917	181.497	190.652	197.391
ε/k (K)	2626.03	2376.05	2398.25	2371.52	2477.31	2558.21
κ_{AB}	0.15532	0.14421	0.11444	0.05324	0.06173	0.07285
M_w	32.042	46.069	60.097	74.123	88.150	102.177

where for the parameters

$$\delta_\tau = 3.4 \times 10^{-2}, \quad \delta_\rho = 5.4, \quad v_1^{(0)} = -4.9 \times 10^{-2}, \quad v_1^{(0)} = 5.0 \times 10^{-3} \tag{26}$$

we adopted the same values as employed by Kiselev and Ely [9] in the simplified crossover SAFT EOS. After this simplification, only two system-dependent parameters, $G_i$and d_1, in Eqs. (17), (18) and (20) are left. In this work, the inverse Ginzburg number $g = 1/G_i$ and the rectilinear diameter amplitude d_1 were represented as linear functions of the molecular weight

$$g = g^{(0)} + g^{(1)} M_w, \qquad d_1 = d_1^{(0)} + d_1^{(1)} M_w \tag{27}$$

where the coefficients

$$g^{(0)} = 18.328, \quad g^{(1)} = 7.06 \times 10^{-3}, \quad d_1^{(0)} = 1.071, \quad d_1^{(1)} = 5.82 \times 10^{-3} \tag{28}$$

are considered as system independent constants for all *n*-alkanols. These constants were found from a fit of the CR SAFT EOS to the VLE and saturated pressure data for methanol and propan-ol-1.

Finally, in the crossover SAFT EOS for *n*-alkanols we have only five adjustable parameters m, v^{00}, u^0/k, ε/k, and κ. We found these parameters from a fit of the crossover SAFT EOS to the experimental saturated pressure, VLE, and one-phase PVT data taken from [14–18] for methanol, from [14,19–21] for ethanol, from [14,22,23] for propan-ol-1, from [14,21,24–26] for butan-ol-1, from [27–31] for pentan-ol-1, and from [27–29,32,33] for hexan-ol-1. The values of all system-dependent parameters of the crossover SAFT EOS for *n*-alkanols are listed in Table 1. Experimental saturated pressure and liquid and vapor density data in comparison with values calculated with the original SAFT and the crossover SAFT EOS are shown in Figs. 1 and 2. The crossover SAFT EOS yields much better description of the VLE data than the original SAFT EOS, especially in the critical region where the SAFT gives up to 20–30% deviations. This is primarily due to the fact that the critical temperatures and pressures calculated with the original SAFT EOS are systematically higher (of about 10–30%) than experimental values. The experimental values of the critical parameters in comparison with the values calculated with the crossover SAFT EOS are listed in Table 2. The maximum deviation of the calculated critical temperature $\Delta T_c = 1.5$ K (or about 0.3%) and the critical pressure $\Delta P_c = 0.11$ MPa (or about 1.5%) is observed for ethanol. For all other *n*-alkanols listed in Table 2 these deviations are less than 0.1% for T_c, and less than 1% for P_c. The calculated critical densities for all *n*-alkanols considered here are about 10% less than the experimental values. However, it does not influence on the quality of description of the VLE data in the critical region. The CR SAFT EOS reproduces the saturated

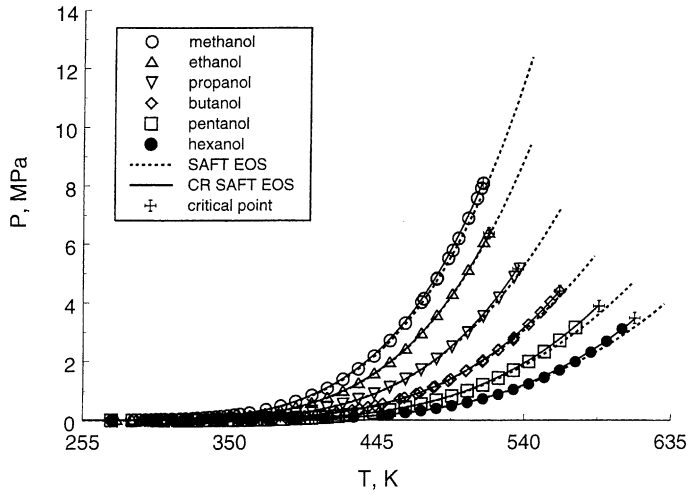

Fig. 1. Saturated pressure data for methanol [14,15], ethanol [14,19,20], propan-1-ol [14,22], butan-1-ol [14,24], pentan-1-ol [27–29], and hexan-1-ol [27–29] (symbols) with predictions of the classical SAFT equation of state (dashed lines) and the crossover SAFT equation of state (solid lines).

pressure with an average absolute deviation (AAD) of about 1% and vapor and liquid density data with AAD of about 3–4% at temperatures $T_c > T \geq 0.99T_c$, and with AAD of about 2% at $T \leq 0.99T_c$.

In comparison to the original SAFT model, the crossover SAFT EOS gives not only a major improvement in the description of VLE data in the critical region, but also yields a better description of the PVT

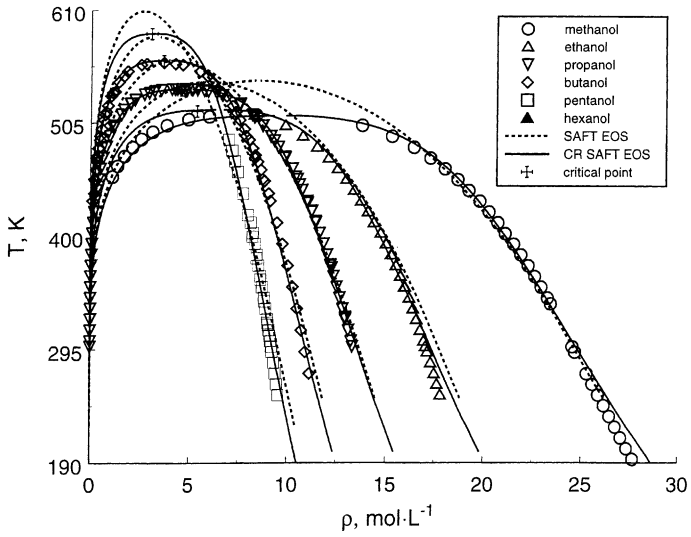

Fig. 2. Saturated density data for methanol [14–17], ethanol [14], propan-1-ol [14,22], butan-1-ol [25,26], pentan-1-ol [27,30], and hexan-1-ol [27,29,32] (symbols) with predictions of the classical SAFT equation of state (dashed lines) and the crossover SAFT equation of state (solid lines).

Table 2
Experimental (exp) and calculated (calc) values of the critical parameters for *n*-alkanols[a]

Parameter	Methanol	Ethanol	Propan-1-ol	Butan-1-ol	Pentan-1-ol	Hexan-1-ol
T_c^{exp} (K)	512.64	516.25	536.71	562.90	588.15	611.40
T_c^{calc} (K)	512.10	517.71	536.67	563.33	588.20	612.28
ρ_c^{exp} (mol l^{-1})	8.475	5.991	4.583	3.650	3.030	2.625
ρ_c^{calc} (mol l^{-1})	9.517	6.452	4.929	3.867	3.270	2.795
P_c^{exp} (MPa)	8.097	6.383	5.170	4.418	3.911	3.510
P_c^{calc} (MPa)	8.114	6.493	5.296	4.450	3.950	3.521

[a] The experimental critical parameters were taken from [34] for methanol, from [29] for ethanol, from [22] for propan-1-ol, from [24] for butan-1-ol, from [18] for pentanol, and from [34] for hexan-1-ol.

data in the one-phase region. Comparisons of the calculated and experimental values of liquid densities for methanol and ethanol are shown in Figs. 3 and 4. Percentage deviations of experimental densities from values calculated with the original SAFT EOS and the crossover SAFT EOS are given in Figs. 5–7. In Fig. 8, we show a comparison between experimental PVT data in the critical and supercritical region of propan-ol-1 with the calculated values. In the one-phase region, the crossover SAFT equation represents the experimental values of pressure with AAD less than 1% in the critical and supercritical region and the liquid densities with AAD of about 2%.

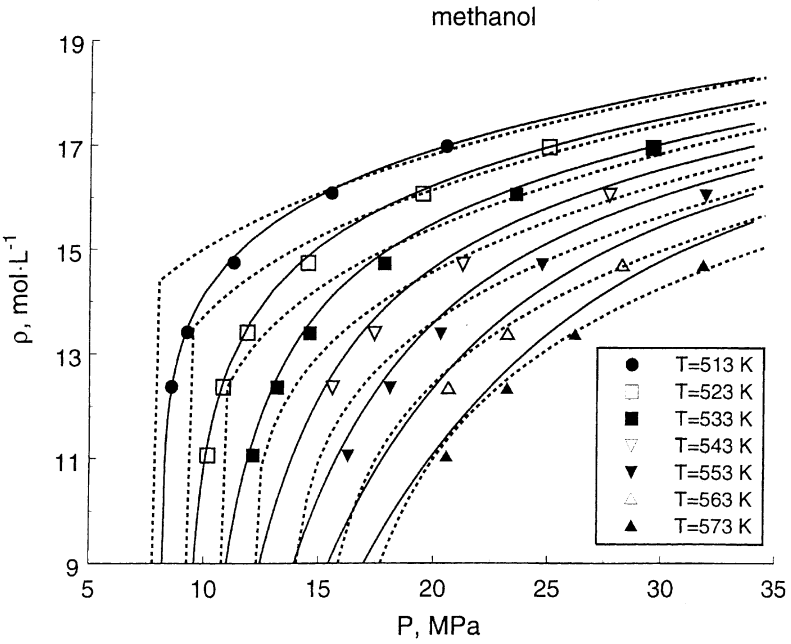

Fig. 3. Liquid density data for methanol [18] (symbols) with predictions of the classical SAFT equation of state (dashed lines) and the crossover SAFT equation of state (lines).

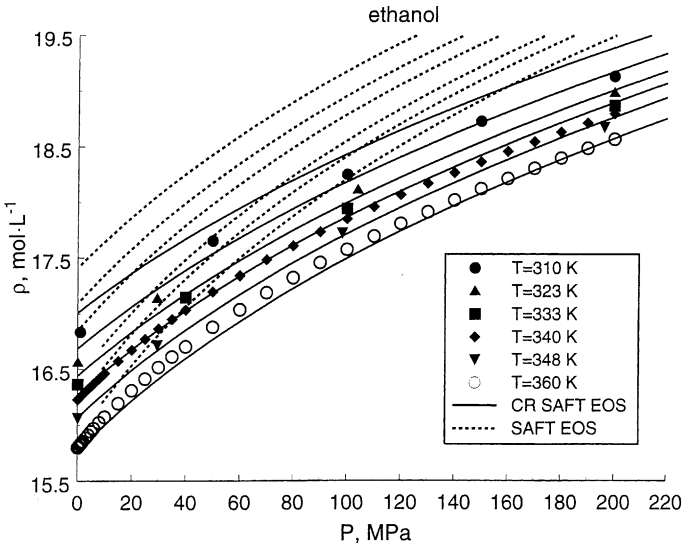

Fig. 4. Liquid density data for ethanol [35] (symbols) with predictions of the classical SAFT equation of state (dashed lines) and the crossover SAFT equation of state (solid lines).

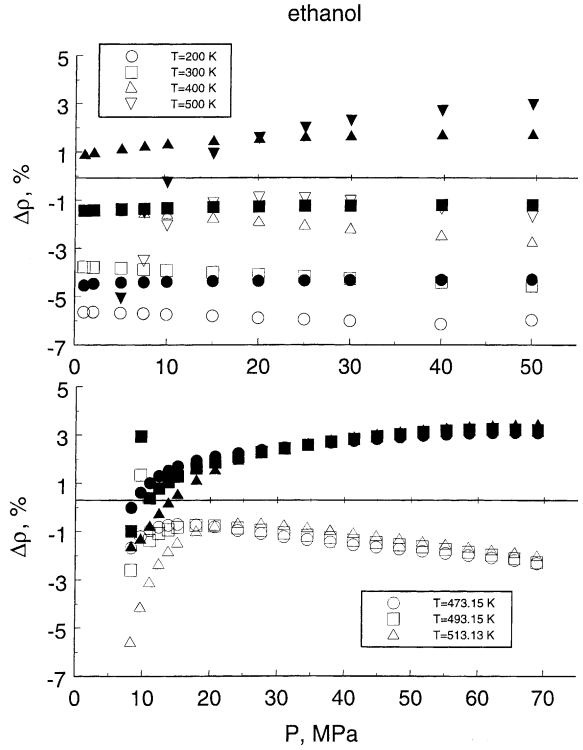

Fig. 5. $P\rho T$ data for propan-1-ol [23] (symbols) with predictions of the classical SAFT equation of state (dashed lines) and the crossover SAFT equation of state (lines).

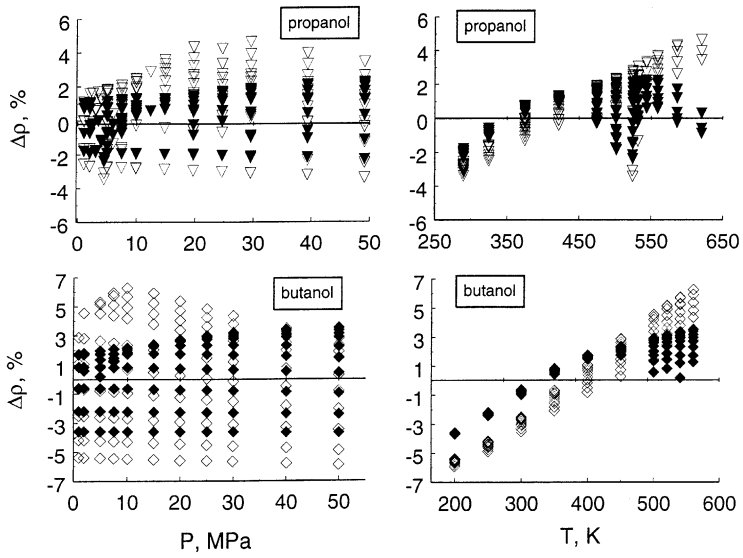

Fig. 6. Percentage deviations of experimental densities for propan-1-ol [23] (top) and butan-1-ol [21] (bottom) from values calculated with the classical SAFT equation of state (empty symbols) and the crossover SAFT equation of state (filled symbols).

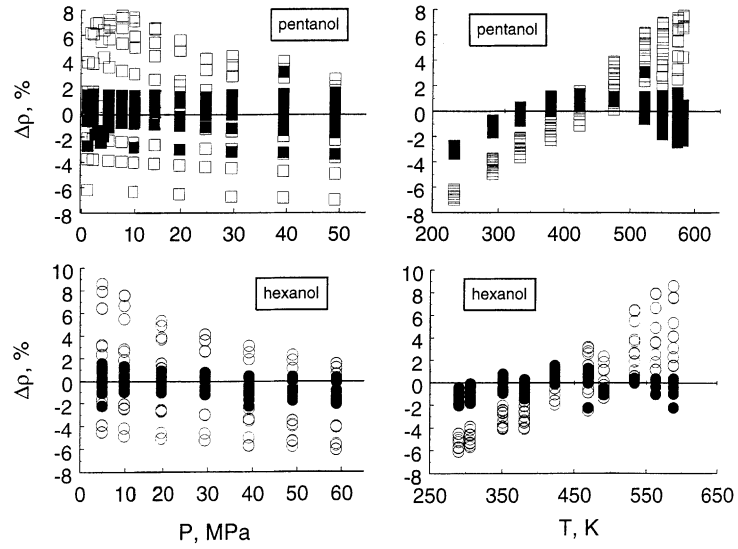

Fig. 7. Percentage deviations of experimental densities for pentan-1-ol [31] (top) and hexan-1-ol [33] (bottom) from values calculated with the classical SAFT equation of state (empty symbols) and the crossover SAFT equation of state (filled symbols).

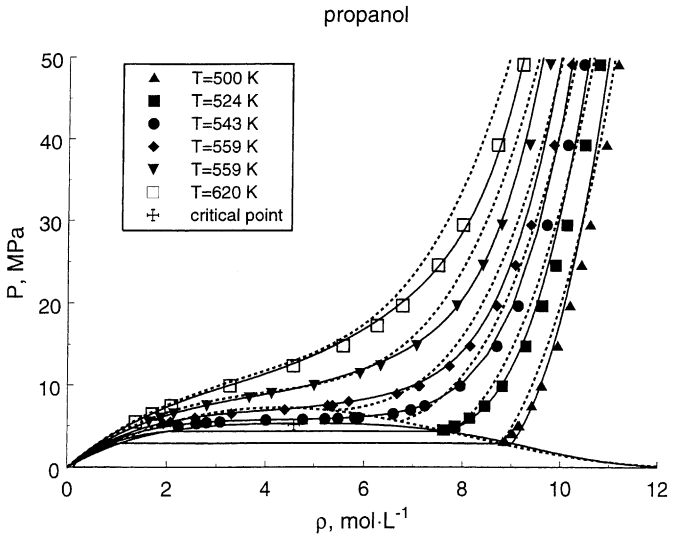

Fig. 8. Percentage deviations of experimental densities of Golubev et al. [21] (top) and of Lo and Stiel [36] (bottom) for ethanol from values calculated with the classical SAFT equation of state (empty symbols) and the crossover SAFT equation of state (filled symbols).

Acknowledgements

The research at the Colorado School of Mines was supported by the US Department of Energy, Office of Basic Energy Sciences, under Grant No. DE-FG03-95ER41568.

References

[1] S.B. Kiselev, J.F. Ely, Ind. Eng. Chem. Res. 38 (1999) 4993–5004.
[2] S.H. Huang, M. Radosz, Ind. Eng. Chem. Res. 30 (1991) 1994–2005.
[3] S.H. Huang, M. Radosz, Ind. Eng. Chem. Res. 29 (1990) 2284–2294.
[4] Y.H. Fu, S.I. Sandler, Ind. Eng. Chem. Res. 34 (1995) 1897–1909.
[5] F.J. Blas, L.F. Vega, Ind. Eng. Chem. Res. 37 (1998) 660–674.
[6] A. Galindo, P.J. Whitehead, G. Jackson, A.N. Burgess, J. Phys. Chem. B 101 (1997) 2082–2091.
[7] M.N. Garcia-Lisbona, A. Galindo, G. Jackson, A.N. Burgess, Mol. Phys. 93 (1998) 57–72.
[8] H. Adidharma, M. Radosz, J. Phys. Chem., submitted for publication.
[9] S.B. Kiselev, J.F. Ely, Fluid Phase Equilib. 174 (2000) 93–113.
[10] N.F. Carnahan, K.E. Starling, J. Chem. Phys. 51 (1969) 635–636.
[11] S.S. Chen, A. Kreglewski, Ber. Bunsen-Ges. Phys. Chem. 81 (1977) 1048–1052.
[12] S.B. Kiselev, Fluid Phase Equilib. 147 (1998) 7–23.
[13] S.B. Kiselev, D.G. Friend, Fluid Phase Equilib. 162 (1999) 51–82.
[14] D. Ambrose, C.H. Sprake, J. Chem. Thermodyn. 2 (1970) 631–645.
[15] W.E. Donham, VLE data for methanol, PhD Thesis, Ohio State University, Columbus, OH, 1953.
[16] V.G. Komarenko, V.G. Manzhelii, A.V. Radtsig, Ukr. Fiz. Zh. 12 (1967) 676–680.
[17] E.W. Washburn, International Critical Tables of Numerical Data, Physics, Chemistry, and Technology, McGraw-Hill, New York, 1926.
[18] R.S. Machado, W.B. Street, J. Chem. Eng. Data 28 (1983) 218–223.

[19] A.F. Gallaugher, H. Hibbert, J. Am. Chem. Soc. 59 (1937) 2514–2521.
[20] K.P. Mishcenko, V.V. Subbotina, Zh. Prikl. Khim. 40 (1967) 1156–1159.
[21] I.F. Golubev, V.k.T.N., Z.V.S., Inzh.-Fiz. Zh. 45 (1980) 668–670.
[22] A.J. Kubicek, P.T. Eubank, J. Chem. Eng. Data 17 (1972) 232–235.
[23] I.F. Golubev, T.N. Vasil'kovskaya, B.C. Zolin, Proc. Trudy GIAP (Russian) 54 (1979) 5–15.
[24] N.B. Vargaftik, Tables on the Thermophysical Properties of Liquids and Gases in Normal and Dissociated States, 2nd Edition, Hemisphere, NY, 1975.
[25] D. Ambrose, R. Townsend, J. Chem. Soc. (1963) 3614–3625.
[26] Y.V. Efremov, Russ. J. Phys. Chem. 40 (1966) 1240–1248.
[27] K.R. Hall, Selected Values of Properties of Chemical Compounds, Thermodynamics Research Center, Texas A&M University, College Station, TX, 1980.
[28] D.R. Stull, Ind. Eng. Chem. 39 (1947) 517–550.
[29] R.C. Wilhoit, B.J. Zwolinski, J. Phys. Chem. Ref. Data 2 (Suppl.1) (1973) 1–483.
[30] J.L. Hales, J.H. Ellender, J. Chem. Thermodyn. 8 (1976) 1177–1184.
[31] V.S. Zolin, I.F. Golubev, T.N. Vasilkovskaya, Trudy GIAP 54 (1979) 22–25.
[32] J. Ortega, J. Chem. Eng. Data 30 (1985) 5–7.
[33] A.A. Gylmanov, T.A. Apaev, L.A. Akhmedov, S.I. Lipovetskii, Izv. Vyssh. Ucheb. Zaved., Neft Gaz 22 (1979) 55–56.
[34] K.R. Hall, TRC Thermodynamic Tables — Nonhydrocarbons, Thermodynamics Research Center, Texas A&M University, College Station, TX, 1987.
[35] Y. Takiguchi, M. Uematsu, Int. J. Thermophys. 16 (1995) 205–214.
[36] H.Y. Lo, L.I. Stiel, Ind. Eng. Chem. Fundam. 39 (1969) 713–718.